



GOLPH3 Promotes Vasculogenic Mimicry via the Epithelial Mesenchymal Transition in Glioblastoma Cells

Jun JIA¹, Liangzhao CHU², Xi ZENG², Niya LONG¹, Minghao DONG², Yushi YANG¹, Yaxin HU¹, Jian LIU¹

¹Guizhou Medical University, College of Clinical Medicine, Guiyang, Guizhou 550004, People's Republic of China

²The Affiliated Hospital of Guizhou Medical University, Department of Neurosurgery, Guiyang, Guizhou 550004, People's Republic of China

Corresponding author: Jian LIU ✉ adamijgray@163.com

ABSTRACT

AIM: To evaluate the relationship between Golgi phosphoprotein 3 (GOLPH3) and vasculogenic mimicry (VM) in glioblastoma cells.

MATERIAL and METHODS: Glioma tissues from 40 glioma patients with different pathological grades were collected. GOLPH3 and VM were evaluated by immunostaining in glioma tissues. Then, the correlation between GOLPH3 and VM were analyzed clinically. Additionally, a GOLPH3-downregulation lentivirus was constructed and transfected into the human primary glioblastoma cell line, U-87 MG. Afterwards, apoptosis, migration and invasion were assessed to determine the effects of downregulation GOLPH3. Then, E-cadherin and matrix metalloproteinase 2 (MMP2) were detected for assessment of the epithelial mesenchymal transition (EMT).

RESULTS: GOLPH3 and VM were found to be positively correlated following clinical analysis ($p < 0.01$, $r = 0.788$). Furthermore, GOLPH3 downregulation suppressed the migration and invasion of U87 MG cells ($p < 0.05$), followed by upregulation of E-cadherin and downregulation of MMP2.

CONCLUSION: Collectively, our results demonstrate that GOLPH3 promoted VM in glioblastoma cells and that the corresponding mechanism was associated with the EMT. Our finding suggests that GOLPH3 may represent a promising therapeutic target for mitigating the recurrence and invasion of gliomas.

KEYWORDS: Glioma, GOLPH3, Vasculogenic mimicry, E-cadherin, Matrix metalloproteinase 2

ABBREVIATIONS: GOLPH3: Golgi phosphoprotein 3, VM: Vasculogenic mimicry, MMP2: Matrix metalloproteinase 2, EMT: Epithelial mesenchymal transition, CD34: Cluster of differentiation 34, PAS: Periodic acid Schiff reaction, shRNA: Short-hairpin RNA, DNA-PK: DNA damage protein kinase, GBM: Glioblastoma multiforme

INTRODUCTION

Gliomas are neuroepithelial tumors, that are often accompanied by genetic mutations such as isocitrate dehydrogenase (IDH), 1p/19q, H₃K₂₇M, V-Rel Reticuloendotheliosis Viral Oncogene Homolog A (RELA), alpha thalassemia/mental retardation syndrome X-linked (ATRX), telomerase reverse transcriptase (TERT), tumor protein P53 (TP53) and B-raf (BRAF) (20). Gliomas are globally recognized as the most common primary malignant brain tumors in adults

and morbidity and mortality rates are increasing each year (17). Gliomas, especially glioblastomas, have a large blood supply, that can be used as a pathological factor to evaluate the prognosis of gliomas (2). Although anti-angiogenic drugs, including bevacizumab, have been demonstrated as promising treatments, results of anti-angiogenic treatments still lack sufficient in clinical efficacies (21).

Conspicuously different from traditional angiogenesis and vasculogenesis, vasculogenic mimicry (VM) is a novel pattern

Jun JIA  : 0000-0002-3994-5015
Liangzhao CHU  : 0000-0003-3418-6117
Xi ZENG  : 0000-0002-7848-7934

Niya LONG  : 0000-0001-8277-5544
Minghao DONG  : 0000-0002-6301-9652
Yushi YANG  : 0000-0003-4699-5894

Yaxin HU  : 0000-0002-4647-6421
Jian LIU  : 0000-0001-8522-5847

of a tumor blood supply without endothelial cells (5). VM was first described by Maniatis et al., who suggested that malignant tumor cells are capable of forming a rich extracellular matrix (ECM) and vasculogenic-like networks (12). Evidence of a clinical pathological connection between VM channels and gliomas has been found, showing that VM channels in gliomas correlate with increasing malignancy and higher aggressiveness (10). Appropriate antagonists have been implicated in VM channel formation in gliomas (14). However, in view of the poor prognosis of glioma patients, further elucidation of VM is needed.

The gene for Golgi phosphoprotein 3 (GOLPH3) is located on chromosome 5 (5p13.3), and GOLPH3 protein has been shown to be evolutionarily conserved (13). Previous studies have revealed that GOLPH3 is an oncogene, and genome-wide analysis of human cancers suggested potential connection between overexpression of GOLPH3 and poor progression of multiple solid tumors (15). Clinical studies have illustrated that the expression of GOLPH3 varies from grades I-III astrocytoma patients to glioblastoma patients (8). Several RNA interferences experiments have demonstrated that the roles of GOLPH3 in proliferation, migration, invasion, differentiation and apoptosis of gliomas *in vitro* remain unclear (1,7,24). Therefore, further elucidation of the roles of GOLPH3 in glioma vascularization is needed. Complex signaling pathways such as phosphoinositide-3-kinase (PI3K)/protein kinase B (AKT)/mammalian target of rapamycin (mTOR), janus kinase (JAK)/signal transducer and activator of transcription 2 (STAT2), wingless-type integration site family (Wnt), mitogen-activated protein kinase (MAPK)/extracellular regulated protein kinases (ERK) and DNA-dependent protein kinase (DNA-PK)/myosin XVIII A (MYO18A) have been reported to have potential relationship with GOLPH3 in the progression of intracranial carcinoma (11,16). Taken together, these findings suggest that GOLPH3 may represent a driver molecule of carcinogenic factors, and may also play a role as a downstream effector through the formation of protein complexes. However, the specific role of GOLPH3 in VM of gliomas has remained unknown.

In the present study, we hypothesized that GOLPH3 may regulate VM and contribute to glioma progression. To this aim, the clinical relationship between GOLPH3 and VM in glioma patients was analyzed. Furthermore, knockdown-GOLPH3 lentiviruses were constructed and transfected into the human primary glioblastoma cell line, U-87 MG, after which we performed several cellular assays *in vitro*.

■ MATERIAL and METHODS

Ethical Approval

The clinical data and tumor specimens of pathologically diagnosed gliomas (WHO I-IV) from patients were collected from April 2019 to April 2020. The clinical procedures and experiments in human primary glioblastoma cell line, U-87 MG, were approved by the Ethics Committee of Guizhou Medical University and its affiliated hospital (IRB-2019-154). All procedures performed in studies related to human participants were in accordance with the 1964 Declaration of Helsinki and its later amendments.

Cell Culture and Groupings

U-87 MG cells were obtained from the Type Culture Collection of the Chinese Academy of Sciences (Shanghai, China). All cells were cultured in Dulbecco's modified Eagle medium supplemented with 10% fetal bovine serum (Hyclone, USA). All cells were cultured in a sterile incubator maintained at 37°C with 5% CO₂. According to the experimental design, the cells were divided into a blank control group, negative control group (NC), and knockdown group (KD).

Clinical Case Collection and Morphological Staining

A total of 40 glioma patients were recruited from the Affiliated Hospital of Guizhou Medical University. Clinical diagnosis by two independent senior pathologists was based on the WHO 2016 classification of the central nervous system. During surgery, the tissues were dissected, fixed in 4% paraformaldehyde solution, routinely sampled, dehydrated, paraffin embedded, and sliced (4 μm). GOLPH3 monoclonal primary antibody (mouse, monoclonal, 1:200; DAKO, USA) was used for immunohistochemical staining. Optical microscopic observation (NIKON, DS-FI2, Japan) and semi-quantitative analysis were performed as follows. The cells in each tissue section were light yellow to brown and these colors served as immuno-positive reaction. Five fields at 400× magnification were randomly selected for each slice. The staining intensity was scored based on the staining characteristics of most cells, as follows: no staining = 0, light yellow = 1, light brown = 2, and brown = 3. The percentage of positive cells was calculated as the average proportion in five fields of view scored as follows: 0~5% = 0, 6%~25% = 1, 26%~50% = 2, 51%~75% = 3, and >75% = 4. The final score for each slice was its score for its staining intensity multiplied by its score for the percentage of positive cells, and final scores were evaluated as follows: 0 was considered to be negative, (-); 1-4 was considered to be weakly positive, (+); 5-8 was considered to be moderately positive, (++) and 9-12 was considered to be strongly positive (+++), as shown in Figure 1A-D. In addition, cluster of differentiation 34 (CD34) primary monoclonal antibody (rat, monoclonal, 1:50; DAKO, USA) and periodic acid Schiff reaction (PAS) were used to assess VM. Briefly, if a cluster of endothelial-like cells (CD34) was negative in five random fields of view, lumen-like or channel structures were observed under a transmitted light microscope, simultaneously combined with PAS-positive staining. VM was identified at 400× magnification. Furthermore, the linear relationship between GOLPH3 and VM was assessed via correlation analysis.

Construction and Transfection of GOLPH3 Lentiviruses

Lentiviruses expressing full-length human GOLPH3 cDNA, as well as lentiviruses carrying short-hairpin RNA (shRNA) against GOLPH3 with an open reading frame RNA (ORF RNA) promoting GOLPH3 were constructed by Shanghai GeneChem (Shanghai, China). The RNA sequence targeting human GOLPH3 was 5'-TAGCATTGAGAGGAAGGTTACA-3'. Viruses were amplified and titrated in 293T cells according to the manufacturer's instructions. Lentiviruses containing empty plasmids (vector) were used as controls. U-87 MG cells were transfected for 72 h and were prepared for further experiments.

Quantitative Real-Time Polymerase Chain Reaction (qRT-PCR)

cDNA was synthesized according to the instructions of the reverse transcriptionTM first-strand cDNA synthesis kit (Thermo Fisher Scientific, USA). Amplification was performed according to FastStart Universal SYBR Green Master (Roche, Switzerland). The reaction parameters set by the PCR instrument as follows: pre-denaturation at 95 °C for 2 min; denaturation at 95 °C for 15 s; annealing for 20 s; and extension at 60 °C for 40 s. A total of 40 cycles were performed. After manual correction, relative expression levels were calculated by 2^{-ΔΔCt} method. The sequences of GAPDH primers were as follows: upstream chain, 5'-TGACTTCAACAGCGACACCCA-3'; and downstream chain, 5'- CACCCTGTTGCTGTAGCCAAA-3'. The sequences of *GOLPH3* primers were as follows: upstream chain, 5'- TAGCATTGAGAGGAAGGTTACA-3'; and downstream chain, 5'- CTGTTGGAGCATCTGACTTAC-3'.

Western Blotting

U-87 MG cells were homogenized in protein extraction reagent (Thermo Fisher Scientific, USA). Specifically, target proteins were subjected to sodium-dodecyl sulfate-polyacrylamide gel electrophoresis and transferred to a polyvinylidene fluoride membrane (Millipore, USA) in transfer buffer. Membranes were blocked with 5% milk and incubated with primary antibody (E-cadherin, mouse, monoclonal, 1:1000, DAKO, USA; MMP2, mouse, monoclonal, 1:500, USA; *GLOPH3*, mouse, monoclonal, 1:500, USA) overnight at 4°C. Horseradish peroxidase-conjugated goat anti-mouse IgG (1:10,000, Thermo Fisher Scientific, USA) antibodies were applied for 2.5 h at 37°C after membranes were washed. Membranes were detected by enhanced chemiluminescence (Millipore, USA) and exposure in the dark. The optical density of each band was measured using Quantity One software (BioRad, USA). Results are reported as the optical density ratio to beta-actin.

Detection of Apoptosis

Apoptosis was detected using the APC Annexin V Apoptosis Detection Kit (Thermo Fisher Scientific, USA) according to the manufacturer's instructions. Briefly, after U-87 MG cells were washed, 100 μL of solution (1×10⁵ cells) was incubated with 5 μL of APC Annexin V for 15 min at 25°C in the dark. The cells were analyzed on a flow cytometer (Bio-Rad, S3TM, USA). Green fluorescent protein (GFP) was directly excited by flow cytometry.

Wound Healing Assays

U-87 MG cells were grown to confluence in six-well plates (Corning, USA). A line by a 1-mL pipette tip was scratched in each hemisphere of the well to wound the cells. During incubation, images were taken of the intersections of the linear cell wound and each grid line at 0, 8, and 24h. The distances between the edges of the wound were measured via imageJ software. Migration rates were calculated using the following equation: (initial distance - final distance/initial distance) × 100. Each test was repeated three times.

Transwell Assays

For invasion assays, the upper chamber was coated with 100 μL of Matrigel (BD, USA). Then, a total of 3 × 10⁵ U-87 MG cells were placed into the upper chamber. The lower chamber was filled with 0.5 mL of medium containing 10% fetal bovine serum. This was followed by incubation at 37°C for 24-48 h. Migrated or invaded cells that attached to the bottom surface of the insert were then fixed with 4% formalin and stained with crystal violet. Each test was repeated three times and nine random fields of view under 200× magnification were analyzed. Penetrated cells were quantified via ImageJ.

Statistical Analysis

IBM SPSS Statistics 20.0 was used for all statistical analysis. All data are reported as the mean ± standard deviation. Chi-square tests (or Fisher's exact tests) were used for determining significant in clinical data. Spearman correlation analysis was performed to determine the linear relationship between *GOLPH3* and VM. Significant differences in the expression levels across group were determined by analysis of variance (ANOVA). p<0.05 or p<0.01 was considered to represent a statistically significant difference.

RESULTS

GOLPH3 and VM are Positively Correlated in Glioma Patients

A univariate log-rank test was used to analyze the relationship between clinical characteristics and *GOLPH3* expression or VM (Table I). The WHO grade I, II, III and IV of glioma patients revealed significantly difference in both *GOLPH3* expression ($\chi^2=14.138$, p<0.01) and VM expression ($\chi^2=7.939$, p<0.01). In contrast, gender, age, and lesion sites were not significantly related to *GOLPH3* or VM expression. In addition, we found that VM was positively correlated with pathological grade (Figure 1E, p<0.01, r=0.854), and *GOLPH3* was also positively correlated with pathological grade (Figure 1F, p<0.01, r=0.852). Furthermore, *GOLPH3* and VM were found to be positively correlated following clinical analysis (Figure 1G, p<0.01, r=0.788).

Successful Construction and Transfection of Knockdown *GOLPH3* Lentiviruses

According to target-tool vector plasmid design, we constructed *GOLPH3*-knockdown GV112 (Figure 2A) plasmids. The target of the *GOLPH3*-knockdown sequence was transfected into U-87 MG cells, and the hairpin structure demonstrated that interference occurred in the target gene sequence (Figure 2B). The results showed expression of *GOLPH3* in cells labeled with GFP (green, Figure 2C), which suggested that knockdown- or overexpression-*GOLPH3* lentiviruses were successfully transfected into host cells. In addition, qRT-PCR results showed that the *GOLPH3* expression ratio was decreased significantly (Figure 2D, p<0.05) in designed KD1 and KD2 plasmids. Considering the corresponding virus titers, KD2 was chosen for further experiments.

Table I: Patients with Clinical Pathological Characteristics (n=40)

Parameters	GOLPH3/n		χ^2	p	VM/n		χ^2	p-value
	Low	High			Low	High		
Gender								
Male	6	16	0.609	0.435	3	19	0.101	0.751
Female	7	11			1	17		
Age (years)								
≥ 50	5	7	0.195	0.658	0	12	0.648	0.421
< 50	8	20			4	24		
Location								
Frontal	3	11	10.08	0.05	1	13	6.876	0.150
Temporal	2	9			0	11		
Parietal	1	1			0	2		
Occipital	1	1			0	2		
>1 lobe	2	5			1	6		
Cerebellum	4	0			2	2		
WHO grade								
I	6	0	14.138	< 0.01*	3	3	7.939	< 0.01*
II	3	11			1	13		
III	1	9			0	10		
IV	3	7			0	10		

* GOLPH3 expression or VM is significantly different in different grades glioma.

Patients with gender, age, tumor location, and tumor pathological grade were analyzed significant differences in GOLPH3 expression and VM expression. Female and male shared no difference in GOLPH3 ($\chi^2=0.609$, $p=0.435$) and VM ($\chi^2=0.101$, $p=0.751$). ≥ 50 and < 50 shared no difference in GOLPH3 ($\chi^2=0.195$, $p=0.658$) and MVD ($\chi^2=0.648$, $p=0.421$). tumor locations shared no difference in GOLPH3 ($\chi^2=10.08$, $p=0.05$) and VM ($\chi^2=6.876$, $p=0.150$). WHO grades shared significantly difference in GOLPH3 ($\chi^2=14.138$, $p<0.01$) and VM ($\chi^2=7.939$, $p<0.01$). * GOLPH3 expression or VM is significantly different in different grades of glioma. n=40. **VM:** Vasculogenic mimicry.

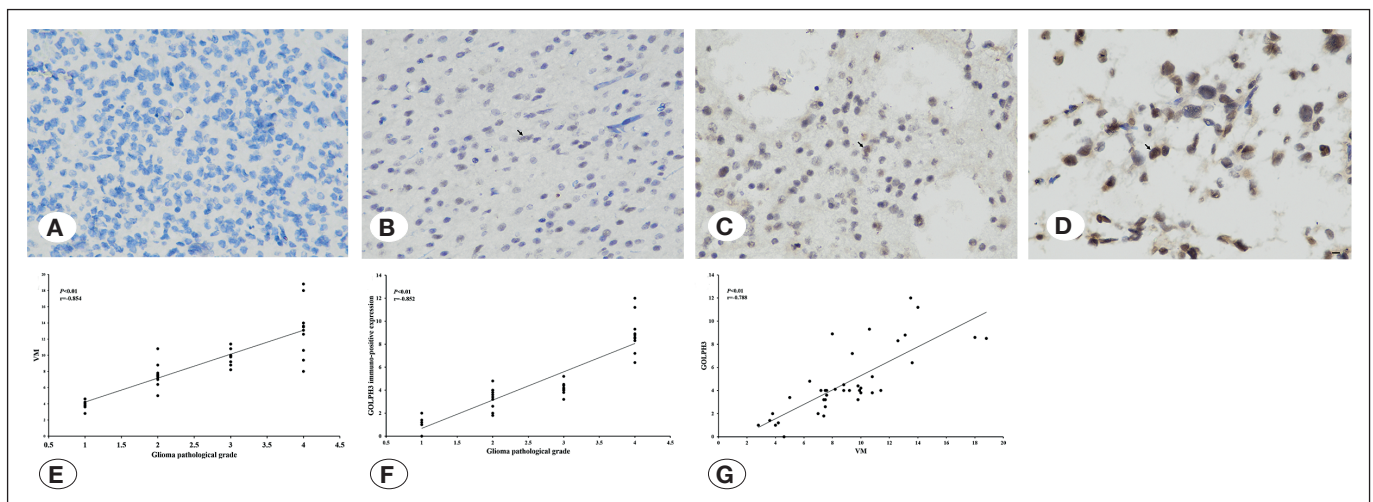


Figure 1: The subcellular localization of GOLPH3 and the pathological grades correlation analysis of GOLPH3 and VM. **A-D)** Were different GOLPH3 subcellular immunostaining intensity following by negative, weak positive, medium positive, and strong positive. The blue was the nucleus, the black arrow indicated the immune-positive cell, and the bar was 400 \times . **E)** Suggested that VM and the pathological grade of glioma were linearly positively correlated. **F)** Suggested that GOLPH3 immune protein expression and the pathological grade of glioma were linearly positively correlated. **G)** Suggested that GOLPH3 and VM were linearly positively correlated in clinical analysis ($p<0.01$).

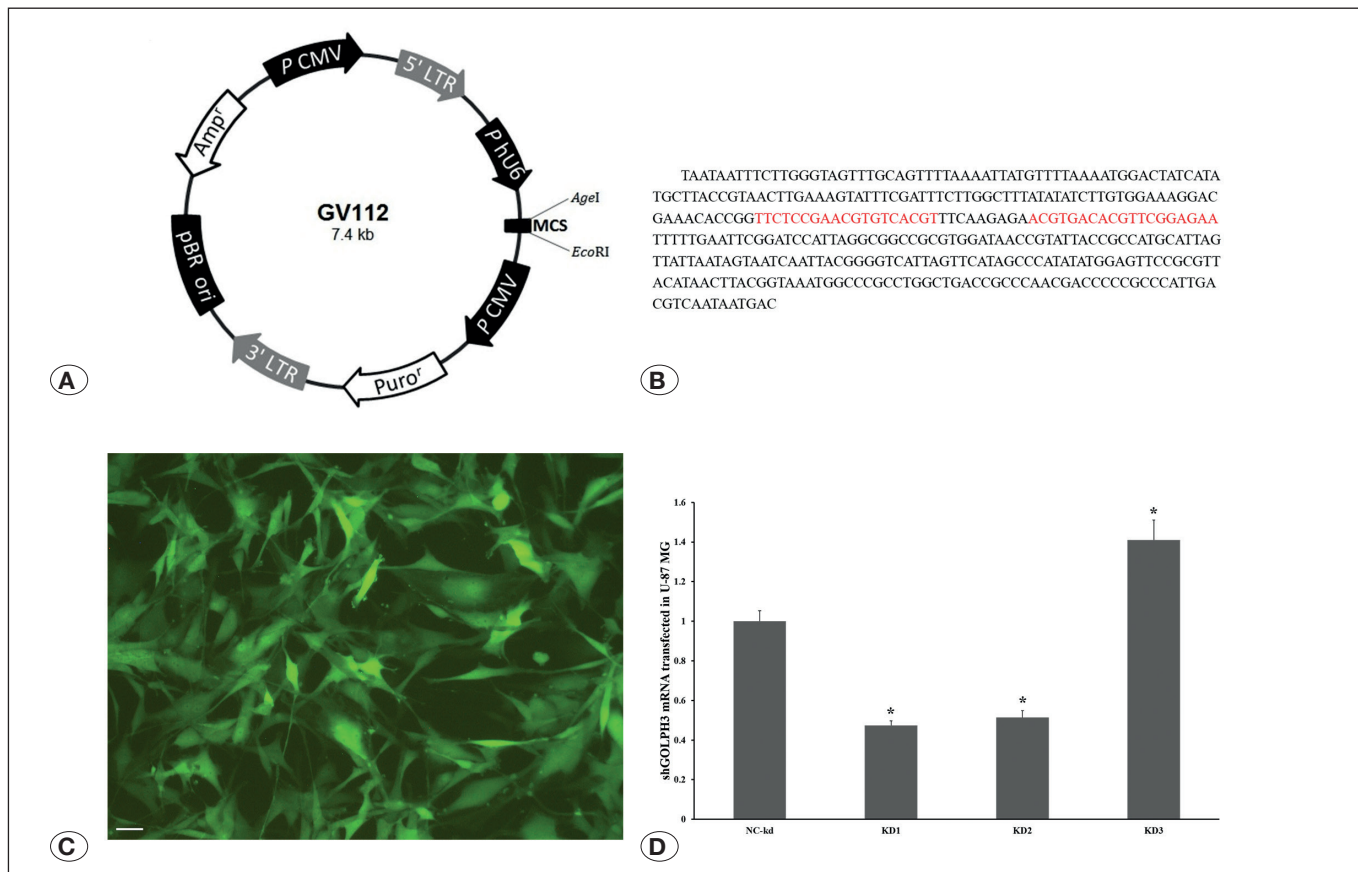


Figure 2: Construction and transfection of GOLPH3 knockdown lentivirus. **A)** Was the schematic of GOLPH3 knockdown lentivirus. element sequence was hU6-MCS-CMV-puro'. Cloning site was *Age* I and *Eco*R I. The framework also contains the antibiotic ampicillin and pBR Ori promoters for vector expression. **B)** Showed the sequencing results after lentivirus transfection. According to the hairpin structure (red) in sequence, GOLPH3 was interfered. **C)** Was fluorescent image of GOLPH3 knockdown lentivirus transfected into U-87 MG cells. The bar was 100 \times . **D)** Showed effective interference of fragment for GOLPH3 inhibition, and the expression of GOLPH3 were downregulated significantly in KD1 and KD2, while were upregulated significantly in KD3 ($p < 0.05$).

Knockdown of GOLPH3 Inhibits the Migration and Invasion of U87 MG Cells

Following knockdown of GOLPH3, we found that the apoptotic rate of each group was less than 5% (Figure 3A-C). In invasion assays, nuclei were observed to exhibit deep-violet staining in each group (Figure 3D-F). Compared with that in the NC group, the invasion effect of the KD group was significantly reduced (Figure 4C, $p < 0.05$). In the migration test, we assessed migration at 0, 8, and 24 h after wounding cells. Since the wound was close to healing at 24 h, the migration distance at 8 h was used to analyze the cell migration rate. The control group was observed under transmitted light (Figure 3G-I), whereas all other groups were observed for GFP fluorescence under a fluorescent microscope (Figure 3J-O). Compared with that of the NC group, the migration effect of KD group was significantly reduced (Figure 4A, $p < 0.05$).

GOLPH3 Regulates the Epithelial Mesenchymal Transition

E-cadherin and MMP2 play an important role in the EMT. After cells were transfected with our GOLPH3-knockdown construct, compared with those of the NC group, we found

that the expression of E-cadherin protein was significantly upregulated (Figure B, D, $p < 0.05$), whereas the expression of MMP2 protein was significantly downregulated (Figure 4B, D, $p < 0.05$).

DISCUSSION

In the present study, clinical glioma tissues were obtained to explore the relationship between GOLPH3 and VM. RNA interference technology was used to construct GOLPH3-knockdown lentiviruses. After transfection of GOLPH3-knockdown lentiviruses in U-87 MG cells, qRT-PCR was used to detect GOLPH3 mRNA levels. Then, flow cytometry, wound healing assays and transwell assays were used to evaluate apoptosis, migration and invasion, respectively. E-cadherin and MMP2 expression levels were detected in all groups. Our results suggested that GOLPH3 and VM were positively correlated in glioma patients. Furthermore, after knockdown of GOLPH3 *in vitro*, apoptosis of U-87 MG cells was not affected, whereas migration and invasion were suppressed. In addition, we found that E-cadherin was upregulated while MMP2 was downregulated following GOLPH3 knockdown.

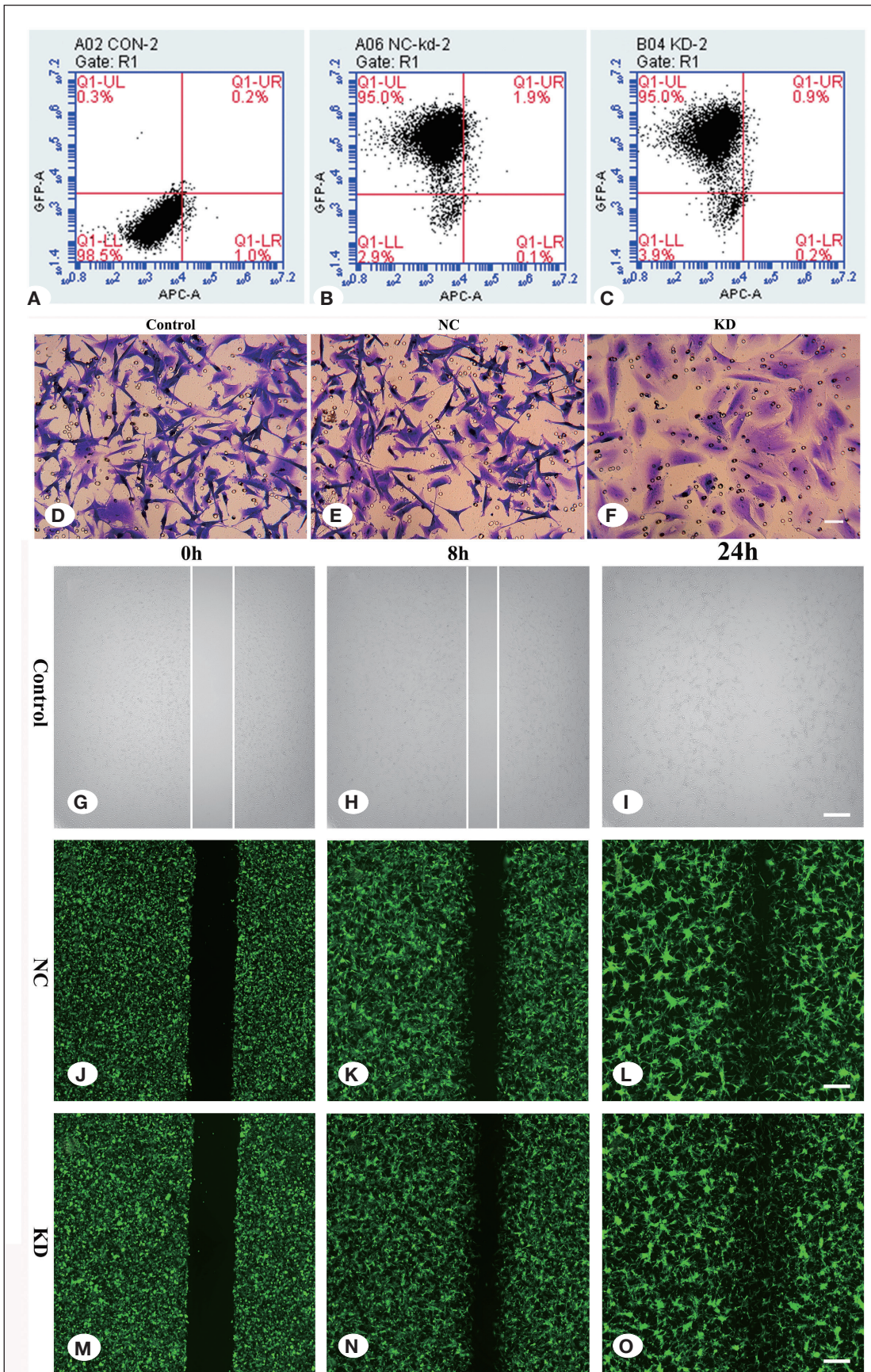


Figure 3: The role of knockdown GOLPH3 in apoptosis, invasion and migration. **A, B) and C)** were apoptosis analysis. No apoptosis in each group. **D, E) and F)** were invasion assay in each group. nucleus was observed with a deep violet. The bar was 200 \times . **G, H) and I)** were 0h, 8h and 24h microscopic observation of cultured cells in white light of control group. The white vertical line was the cell migration boundary. The bar was 100 \times . **J-O)** were 0h, 8h and 24h microscopic observation of cultured cells in green fluorescence of NC group and KD group. The bar was 100 \times .

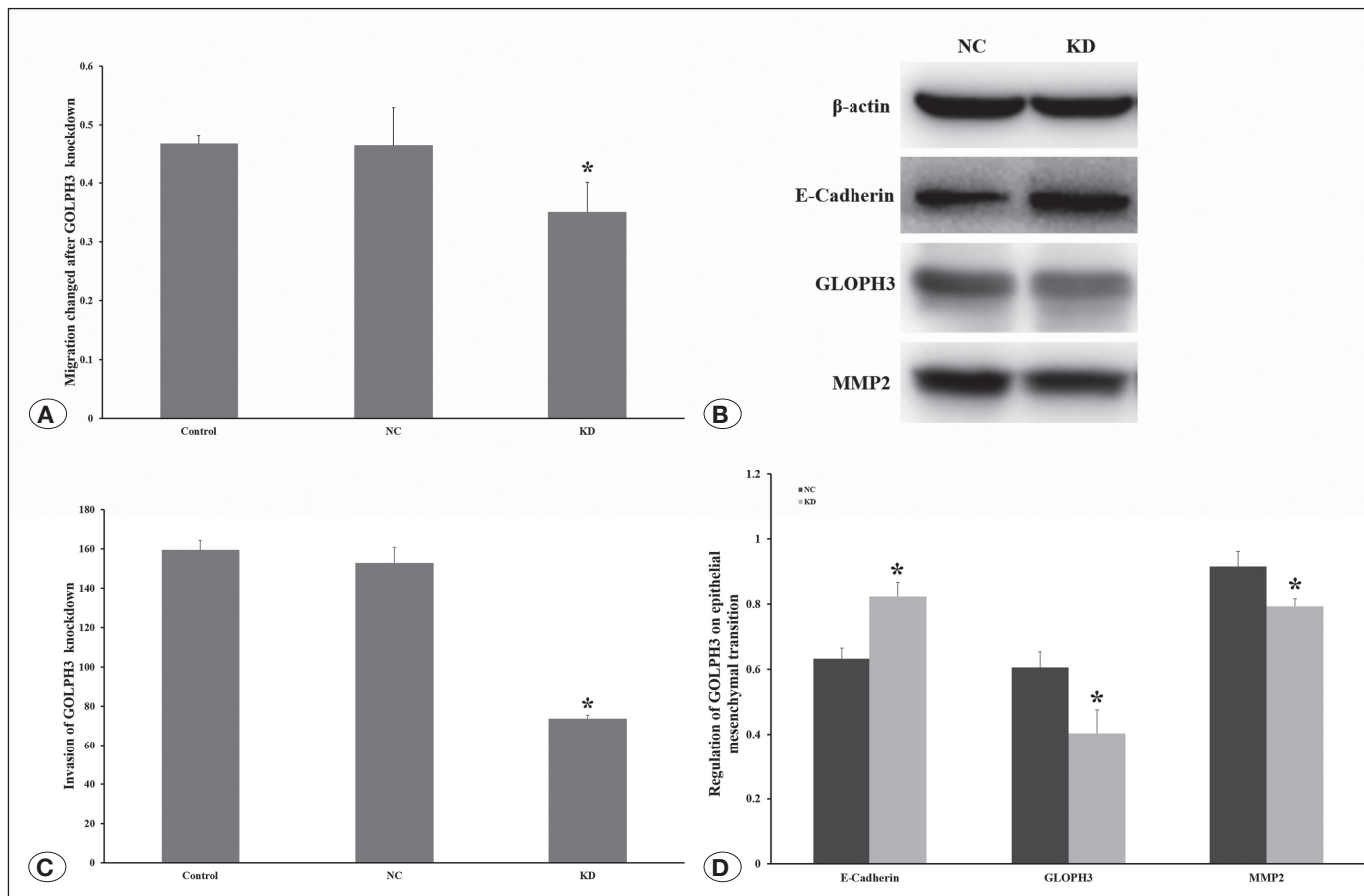


Figure 4: Regulation of GOLPH3 on epithelial mesenchymal transition. **A)** Was migration change after GOLPH3 knockdown. Compared with NC group, the migration effect of KD group was significantly downregulated ($p < 0.05$). **B)** Showed the western blot bands of the proteins associated with epithelial mesenchymal transition in vitro, including E-Cadherin and MMP2. β -actin was an internal reference. **C)** Was invasion of GOLPH3 knockdown. Compared with NC group, the invasion effect of KD group was significantly downregulated ($p < 0.05$). **D)** After GOLPH3 was inhibited, GOLPH3 protein was down-regulated significantly ($p < 0.05$). Meanwhile, compared with the NC group, the gray value of E-Cadherin in KD group was up-regulated ($p < 0.05$), but the gray value of MMP2 was down-regulated ($p < 0.05$).

During vesicular trafficking in the Golgi apparatus, GOLPH3 has been shown to bind to PI4P (13). Additionally, DNA damage protein kinase (DNA-PK) is stimulated by DNA damage, at which time it phosphorylates GOLPH3 on Thr143 and Thr148 to enhanced interaction between GOLPH3 with MYO18A (24). This strong bridging effect connects *trans*-Golgi PI4P-rich domains with the actin cytoskeleton, thus generating a tensile force causing Golgi dispersal and fragmentation. Increased fragmentation of the Golgi apparatus has been correlated with the development and maintenance of cancer cells (4). Furthermore, GOLPH3 is considered to be an oncogene. In our present study, we found that the expression of GOLPH3 was upregulated with the pathological grade of glioma in the tested patients. Remarkably, Choi et al. (3) reported that DNA repair mechanisms and the EMT were reversed in glioblastoma multiforme (GBM) cells. Combined with our present experimental results, these findings suggest that the EMT and GOLPH3 are implicated in the mechanisms of glioma progression.

The EMT is critical for cancer cell migration and invasion. Wen et al. (19) found that knockdown of GOLPH3 in an endometrial carcinoma cell line inhibited N-cadherin and vimentin, and stimulated E-cadherin and α -catenin, all of which associated with the EMT. Additionally, Tan et al. (18) demonstrated that the scaffolding protein, PITPNC1, Golgi apparatus of lung adenocarcinoma cell lines contributed to EMT. Moreover, knockdown of GOLPH3 has been shown to block the effects of PITPNC1 overexpression (6), indicating that PITPNC1 acts through GOLPH3. Interestingly, the results of our present study revealed that GOLPH3 downregulation in U-87 MG cells inhibited migration and invasion, suggesting that GOLPH3 may contribute to the EMT in glioma cells. What's more, Ling et al. (9) reported that inhibition of the EMT impaired VM in glioma via the p38/MAPK signaling pathway. In addition, Zhang et al. (23) illustrated that LRIG1 inhibited VM via the EMT, highlighting an interaction between VM and the EMT in the progression of gliomas. Moreover, in our present study, knockdown of GOLPH3 promoted the expression of E-cadherin and inhibited the expression of MMP2 in glioma

cells, suggesting that GOLPH3 regulates the EMT and correspondingly leads to glioma VM.

However, some results of our present study were inconsistent with those of previous studies. After GOLPH3 overexpression, the mTOR/ YB1 pathway has been shown to be activated and migration and invasion of glioma cells are increase (22). Furthermore, overexpression of GOLPH3 *in vitro* promotes growth via the PKD2/GOLPH3/AKT pathway (25). Since high GOLPH3 expression has been shown to be clinically associated with GBM patients (8,24), previous studies and present study may have assessed different microenvironments and employed different experimental conditions. In addition, a previous study reported that GOLPH3 siRNA-transfected U-251 cells and U-87 cells showed higher rates of apoptosis, whereas GOLPH3 downregulation did not significantly affect apoptosis in our present study. The disadvantage of this article is that there are too few clinical samples. The sample is not linked to the survival time of the relevant patient. Some negative results in the experiment are inconsistent with previous reports and cannot be explained temporarily.

CONCLUSION

Taken together, our present findings suggest that GOLPH3 promoted VM in glioblastoma cells and that the related mechanisms were associated with the EMT. Hence, GOLPH3 may represent a promising therapeutic target for ameliorating the recurrence and invasion of glioma.

ACKNOWLEDGEMENTS

The authors would like to thank the included patients who allowed for their glioma tissues to be studied.

We thank LetPub (www.letpub.com) for its linguistic assistance during the preparation of this manuscript.

AUTHORSHIP CONTRIBUTION

Study conception and design: JL
 Data collection: XZ
 Analysis and interpretation of results: MD
 Draft manuscript preparation: JJ
 Critical revision of the article: LC
 Investigation and Formal analysis: NL, YY
 Resources and Visualization: YH
 All authors (JJ, LC, XZ, NL, MD, YY, YH, JL) reviewed the results and approved the final version of the manuscript.

REFERENCES

- Arriagada C, Luchsinger C, González AE, Schwenke T, Arriagada G, Folch H, Ehrenfeld P, Burgos PV, Mardones GA: The knocking down of the oncoprotein Golgi phosphoprotein 3 in T98G cells of glioblastoma multiforme disrupts cell migration by affecting focal adhesion dynamics in a focal adhesion kinase-dependent manner. *PloS one* 14(2): e0212321, 2019
- Berntsen EM, Stensjøen AL, Langlo MS, Simonsen SQ, Christensen P, Moholdt VA, Solheim O: Volumetric segmentation of glioblastoma progression compared to bidimensional products and clinical radiological reports. *Acta Neurochirurgica* 162(2):379-387, 2020
- Choi EJ, Cho BJ, Lee DJ, Hwang YH, Chun SH, Kim HH, Kim IA: Enhanced cytotoxic effect of radiation and temozolomide in malignant glioma cells: Targeting PI3K-AKT-mTOR signaling, HSP90 and histone deacetylases. *BMC Cancer* 14:17, 2014
- Farber-Katz SE, Dippold HC, Buschman MD, Peterman MC, Xing M, Noakes CJ, Tat J, Ng MM, Rahajeng J, Cowan DM, Fuchs GJ, Zhou H, Field SJ: DNA damage triggers Golgi dispersal via DNA-PK and GOLPH3. *Cell* 156(3):413-427, 2014
- Folberg R, Hendrix MJ, Maniotis AJ: Vasculogenic mimicry and tumor angiogenesis. *Am J Pathol* 156(2):361-381, 2000
- Halberg N, Sengelaub Caitlin A, Navrazhina K, Molina H, Uryu K, Tavazoie S: PTPN13 recruits RAB1B to the Golgi network to drive malignant secretion. *Cancer Cell* 29:339-353, 2016
- Li X, Li M, Tian X, Li Q, Lu Q, Jia Q, Zhang L, Yan J, Li X, Li X: Golgi phosphoprotein 3 inhibits the apoptosis of human glioma cells in part by downregulating N-MYC downstream regulated gene 1. *Med Sci Monit* 22:3535-3543, 2016
- Li XY, Liu W, Chen SF, Zhang LQ, Li XG, Wang LX: Expression of the Golgi phosphoprotein-3 gene in human gliomas: A pilot study. *J Neuro-Oncol* 105(2):159-163, 2011
- Ling G, Ji Q, Ye W, Ma D, Wang Y: Epithelial-mesenchymal transition regulated by p38/MAPK signaling pathways participates in vasculogenic mimicry formation in SHG44 cells transfected with TGF- β cDNA loaded lentivirus in vitro and in vivo. *Int J Oncol* 49(6):2387-2398, 2016
- Liu XM, Zhang QP, Mu YG, Zhang XH, Sai K, Pang JC, Ng HK, Chen ZP: Clinical significance of vasculogenic mimicry in human gliomas. *J Neuro-Oncol* 105(2):173-179, 2011
- Lu D, Zhang H, Fu J, Qi Y, Wang X, Wu S, Zhou X, Yu R: Golgi phosphoprotein 3 promotes WIs recycling and Wnt secretion in glioma progression. *Cell Physiol Biochem* 47(6):2445-2457, 2018
- Maniotis AJ, Folberg R, Hess A, Seftor EA, Gardner LM, Pe'er J, Trent JM, Meltzer PS, Hendrix MJ: Vascular channel formation by human melanoma cells in vivo and in vitro: Vasculogenic mimicry. *Am J Pathol* 155(3):739-752, 1999
- Nakashima-Kamimura N, Asoh S, Ishibashi Y, Mukai Y, Shidara Y, Oda H, Munakata K, Goto Y, Ohta S: MIDAS/GPP34, a nuclear gene product, regulates total mitochondrial mass in response to mitochondrial dysfunction. *J Cell Sci* 118(Pt 22): 5357-5367, 2005
- Plate KH, Scholz A, Dumont DJ: Tumor angiogenesis and anti-angiogenic therapy in malignant gliomas revisited. *Acta Neuropathologica* 124(6):763-775, 2012
- Scott KL, Kabbarah O, Liang MC, Ivanova E, Anagnostou V, Wu J, Dhakal S, Wu M, Chen S, Feinberg T, Huang J, Saci A, Widlund HR, Fisher DE, Xiao Y, Rimm DL, Protopopov A, Wong KK, Chin L: GOLPH3 modulates mTOR signalling and rapamycin sensitivity in cancer. *Nature* 459(7250):1085-1090, 2009

16. Sechi S, Frappalo A, Karimpour-Ghahnavieh A, Piergentili R: Oncogenic roles of GOLPH3 in the physiopathology of cancer. *Int J Mol Sci* 21(3):933, 2020
17. Siegel RL, Miller KD, Jemal A: Cancer statistics, 2020. *CA: A Cancer Journal for Clinicians* 70(1):7-30, 2020
18. Tan X, Banerjee P, Guo HF, Ireland S, Pankova D, Ahn YH, Nikolaidis IM, Liu X, Zhao Y, Xue Y, Burns AR, Roybal J, Gibbons DL, Zal T, Creighton CJ, Ungar D, Wang Y, Kurie JM: Epithelial-to-mesenchymal transition drives a pro-metastatic Golgi compaction process through scaffolding protein PAQR11. *J Clin Invest* 127(1):117-131, 2017
19. Wen Y, Tan X, Wu X, Wu Q, Qin Y, Liang M, Ran G, Gu H, Xie R: Golgi phosphoprotein 3 (GOLPH3) promotes endometrial carcinoma cell invasion and migration by regulating the epithelial-mesenchymal transition. *Cancer Biomark* 26(1):21-30, 2019
20. Wesseling P, Capper D: WHO 2016 Classification of gliomas. *Neuropathol Appl Neurobiol* 44(2):139-150, 2018
21. Wick W, Platten M, Wick A, Hertenstein A, Radbruch A, Bendszus M, Winkler F: Current status and future directions of anti-angiogenic therapy for gliomas. *Neuro-Oncology* 18(3):315-328, 2016
22. Zhang X, Ding Z, Mo J, Sang B, Shi Q, Hu J, Xie S, Zhan W, Lu D, Yang M, Bian W, Zhou X, Yu R: GOLPH3 promotes glioblastoma cell migration and invasion via the mTOR-YB1 pathway in vitro. *Mol Carcinog* 54(11):1252-1263, 2015
23. Zhang X, Song Q, Wei C, Qu J: LRIG1 inhibits hypoxia-induced vasculogenic mimicry formation via suppression of the EGFR/PI3K/AKT pathway and epithelial-to-mesenchymal transition in human glioma SHG-44 cells. *Cell Stress & Chaperones* 20(4):631-641, 2015
24. Zhou J, Xu T, Qin R, Yan Y, Chen C, Chen Y, Yu H, Xia C, Lu Y, Ding X, Wang Y, Cai X, Chen J: Overexpression of Golgi phosphoprotein-3 (GOLPH3) in glioblastoma multiforme is associated with worse prognosis. *J Neuro-Oncol* 110(2):195-203, 2012
25. Zhou X, Xue P, Yang M, Shi H, Lu D, Wang Z, Shi Q, Hu J, Xie S, Zhan W, Yu R: Protein kinase D2 promotes the proliferation of glioma cells by regulating Golgi phosphoprotein 3. *Cancer Letters* 355(1):121-129, 2014